FEM Analysis of effects of mechanical impact parameters on fruit characteristics

Emanuele Cerruto[1*], Claudia Aglieco[1], Klaus Gottschalk[2],

Jelena Surdilovic[2], Giuseppe Manetto[1], Martin Geyer[2]

(1. Department of Agricoltura, Alimentazione e Ambiente (Di3A) – University of Catania, Italy;

2. Leibniz-Institut für Agrartechnik Potsdam-Bornim e.V. (ATB), Potsdam, Germany)

Abstract: Mechanical impact on fresh agriculture commodities may be a criterial issue during mechanical processes such as grading, sorting, conveying, packing or transport. The applications of electronic measuring devices in form of artificial fruits like 'Instrumented Spheres' (IS) are an aid to quantify influences of mechanical impact on the value of fruit, vegetable and potato. Additionally, modelling and simulation of impact on fruits help to identify those influencing parameters. In this study, modelling and simulation runs were performed based on the Finite Element Method (FEM). The relevant parameters modulus of Young, density, mass, fruit dimensions, and dropping test heights were varied for the simulation tests. FEM simulation results were compared with measured acceleration values and impact force values and obtained in a previous work from dropping potato tuber tests, by using a force sensor and an 'Acceleration Measuring Unit' (AMU). The AMU can be implemented into real or artificial fruits to measure the acceleration upon impact. From previous work it was found that, when dropping potato tubers with mass of 100 120 g from 25 cm height onto steel plates, the impact force ranged from 190 to 220 N. Simulations showed that the impact force in similar conditions (mass of 102 113 g and modulus of Young of 2.5 3.5 MPa) ranged from 198 to 242 N, which is in good agreement with the experimental results. When the tuber mass was 190 210 g, the measured impact force varied from 310 to 325 N. Simulations for masses of 199–221 g resulted in impact forces of 306 325 N, again in good agreement with the experimental results. However, AMU acceleration values ranged from 922 932 m/s^2 for masses of 100 120 g to 765 824 m/s2 for masses of 190 210 g. Simulations, in similar conditions, provided acceleration values of 1934 2314 m/s^2 for masses of 102 113 g (modulus of Young 2.5 3.5 MPa) and ranging from 1497 to 1843 m/s^2 for masses of 199 221 g, which are about twice higher than measured, probably due to effects from imperfect fit when the AMU was implanted into the test fruit.

Keywords: Post-harvest, fruit damage, impact force, impact acceleration, FEM.

1   Introduction

Harvest, transport and post-harvest handling expose fruits and vegetables to numerous mechanical impacts. As an example, studies on orange packing lines involving feeding, pre-selection, pre-washing, washing, waxing, drying, selection, calibration and packing have shown that an orange is on average subjected to over 60

impacts of an intensity greater than 19 *g* (1 *g* = 9.81 m/s^2) (Blandini et al., 2003). These impacts may cause damage such as texture destruction, so reducing the quality and the commercial value of the fruits, resulting in severe economic losses (Baritelle and Hyde, 2001; Bielza et al., 2003; Idah et al., 2012; Eissa et al., 2013).

There are numerous technologies available for bruise measurement (Studman, 2001; Opara and Pathare, 2014), including near infrared spectroscopy, hyperspectral imaging, thermal imaging, nuclear magnetic resonance imaging, optical measurement systems, acoustic methods and use of electrical characteristics and biosensors.

Moreover, several "artificial fruits" (Instrumented Spheres – IS) which mimic the physical properties and mechanical responses of fruits and vegetables during post-harvest handling have been designed and marketed. Essentially, they are data loggers subjected to the same mechanical stress as real products, mainly used to evaluate the effect of transfer height, velocity, belt structure and padding on fruit bruising susceptibility in packing lines (Ortiz-Cañavate et al., 2001; Shahbazi et al., 2011; Praeger et al., 2013). Mechanical stresses are recorded in terms of acceleration, using accelerometers as in IS100 (Zapp et al., 1990; Ragni and Berardinelli, 2001; Di Renzo et al., 2009) and PTR 100 (or PTR 200) (Van Canneyt et al., 2003), or in terms of forces using pressure measuring sensors as in PMS 60 (Herold et al., 1996).

All these instrumented devices are frequently used to locate those zones in the harvesting and processing chain that present a high level of risk of damage. They measure the actual mechanical impacts at different processing steps and can thus be helpful in identifying the potential risks of mechanical damage and in evaluating measures to reduce impact loads.

Their greatest drawback is mainly due to the considerable differences between real and artificial fruit, largely restricting the transferability of measured impact data (force or acceleration) to real products.

A miniaturised Acceleration Measuring Unit (AMU) has been recently developed at the Leibniz-Institut für Agrartechnik Potsdam-Bornim (ATB) (Figure 1). When implanted into a real product like a potato tuber, it is able to measure, at the centre of the fruit, the accelerations deriving from an impact (Geyer et al., 2009). Nevertheless, the implantation procedure of the AMU inside the tuber affected the reproducibility of measurement. Further studies are necessary.
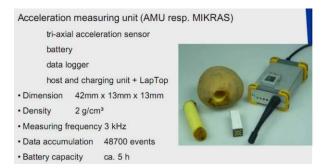

Figure 1 AMU for implementation into real or dummy fruit bodies (Geyer et al, 2009).

In this research a different approach was exploited, based on the Finite Element Method (FEM). FEM analysis is largely applied to simulate collision fruit-to-fruit or fruit-to-rigid walls (Dintwa et al., 2008). Mechanical stress is propagating inside the tissue material upon external (punctual) impact and has local different distribution usually. The FE-Method is useful to simulate and analyse such effects depending on material properties, fruit shape and dimensions, and load conditions. FEM simulation can help to understand such phenomena and to acquire conditions to reduce damage and bruises.

The impact parameters usually used to analyse post-harvest damage are acceleration and impact force. Therefore, an elementary FEM model of a fruit, based on elastic linear behavior of the material, was developed with the main objective of evaluating the effects of size and main physical properties of the fruit on acceleration and impact force.

2 Material and methods

2.1 Preliminary tests

Some preliminary drop tests were carried out to gather reference data that can be useful to assess the response of the model. They were executed by using two spherical artificial fruits and the drop simulator represented in Figure 2, the same used by Geyer et al. (2009) for potato tubers drop tests with the AMU device.
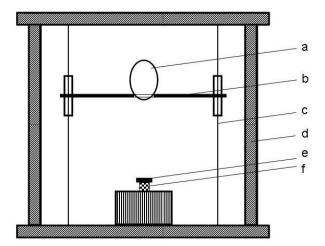
Figure 2 Schematic view of the drop simulator (Geyer *et al.*, 2009): a = artificial fruit, b = sliding carriage, c = guide wire, d = frame, e = steel plate, and f = force sensor.

Figure 3 The two artificial fruits (left = AF 1; right = AF 2) used for preliminary drop tests.

Table 1 Main features of the two artificial fruits

Artificial fruit (AF)	Diameter, mm	Mass, g	Density, kg/m³	Modulus of Young, MPa
AF 1	68.4	57	338	4.3-5.6
AF 2	57.4	134	1350	21.3-30.5

It consists of a frame with two vertical guide wires, taut clamped in parallel. A sliding carriage which is free to move along the guide wires, has a circular hole in its middle. An artificial fruit, placed on the carriage, protrudes slightly from the hole, depending on its radius of curvature. The diameter of the hole (40 mm) is wider than that of a circular plate (30 mm), rigidly coupled to a force sensor at the bottom of the frame. So, when the carriage slides along the wires, the fruit only hits the circular plate coupled to the force sensor and the impact force is measured.

The two artificial fruits used for the drop tests are shown in Figure 3 and their main characteristics are reported in Table 1. The values of the modulus of Young were calculated on the basis of the Hertz theory by using a texture analyser instrument that measures the deformations produced by given forces (ASAE Standard, 1999). The coefficient of Poisson was assumed equal to 0.49, as in potato tubers (Mohsenin, 1986). On the other hand, the error in modulus of Young estimation introduced by assuming an approximate value of the coefficient of Poisson, would be minimal (Rao et al., 2005).

Drop tests were carried out from 10 and 25 cm height; the impact surface was a steel plate and steel covered with 5 mm of PVC.

2.2 Model building

FEM simulations were developed by using the Salome-Meca and Code-Aster software packages contained in the Linux distribution CAElinux 2011 (http://www.caelinux.com). Salome-Meca is an open-source software that provides a generic platform for pre- and post-processing for numerical simulations. The platform has been built using a collaborative development approach and it is therefore available under the LGPL license (http://www.salome-platform.org). Code-Aster is mainly a solver for mechanics, based on the theory of finite elements. This tool also covers a wide range of applications for civil and structural engineering. Originally developed as an in-house application by the French company EDF, it was released under the terms of the GNU General Public License in October 2001 and can be freely obtained at its official website (http://www.code-aster.org).

Salome-Meca was used as a standalone application for generation of the CAD model and its preparation for numerical calculations (meshing). The geometry of the model reproduced that of the drop simulator: a sphere dropping onto a cylindrical plate (Figure 4). Meshing was performed by using tetrahedron-shaped elements.
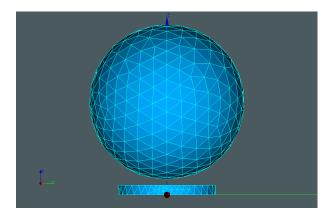
Figure 4 Geometric model used for drop tests after meshing.

Preliminary simulations were carried out reproducing the drop tests from 10 and 25 cm with the artificial fruits. The impact plate was modelled as a steel cylinder (height = 5 mm, diameter = 30 mm, modulus of Young = 210000 MPa; density = 7800 kg/m^3; coefficient of Poisson = 0.27) and the artificial fruits as spheres with the features reported in Table 1.

Material properties and geometrical constraints were applied within Code-Aster. Instructions were given in a script Python file, whose main parts regarded:

• Assignment of material properties to the objects;

• Assignment of boundary conditions: no displacements for the base of the cylindrical plate;

• Definition of the contact conditions between sphere and cylinder (plate): Formulation = "Discrete", Algorithm = "Lagrangian";

• Solution of the equations and calculation of stresses, displacements and nodal forces: in this first step of the research, material behaviour was considered elastic linear;

• Extraction of the acceleration at the centre of the sphere and of the impact force on the base of the cylindrical plate.

2.3 Experimental plan and data analyses

Preliminary simulations were in good agreement with experimental results from drop tests carried out with artificial fruits: the relative error on the impact force on steel surface ranged from about -3% up to 2%. So, the model was extensively used for an analysis on the effects of drop height, diameter, density and modulus of Young of the fruit on impact force and acceleration at the centre of the fruit. In this first study, the acceleration sensor was not simulated inside the fruit.

In detail, the experimental plan considered:

a)   sphere diameter D: 50, 55, 60, 65, 70, 75 and 80 mm;

b)   modulus of Young E: 0.5, 1.5, 2.5 and 3.5 MPa;

c)   material density ρ: 900, 1000 and 1100 kg/m^3;

d)   drop height h: 10, 15, 20, 25, 35 and 50 cm.

With the given values of material density and sphere diameter, the mass of the sphere ranged from 59 up to 295 g. The coefficient of Poisson was kept unchanged across all the simulation tests (0.49). All values for simulations were chosen to approach potato tubers properties (Bentini et al., 2008; Geyer et al., 2009).

Meshing was performed by using tetrahedron-shaped elements, keeping constant the maximum linear dimensions for mesh cells (10 mm) and applying a local refinement at the centre of the sphere (5 mm). So, the cylindrical plate was characterised by 252 nodes, 74 edges, 478 faces and 672 volumes. The corresponding values for the sphere, when the diameter ranged from 50 mm up to 80 mm, were 334–765 nodes, 14–15 edges, 570–600 faces and 1357–3474 volumes. The chosen mesh size was a compromise between computing performance needed and calculation accuracy. More refined mesh influence will not result in much significant accuracy improvement for this study.

The following quantities were extracted from each run test:

a)   the maximum impact force transmitted to the steel plate (corresponding to that measured by the force sensor during drop tests);

b)   the maximum acceleration at the centre of the sphere (corresponding to that measured by the AMU device).

Globally, 360 simulations were carried out. Acceleration and impact force were analysed at varying the model parameters: diameter, density, mass, modulus of Young of the sphere and drop height. Data analyses and graphical representations were carried out by using the software *R* (R Core Team, 2013).

3 Results and discussion

3.1 Effect of drop height

Figure 5 reports the maximum impact force trend vs. the drop height at varying density and modulus of Young of the material for three sphere diameters. Similar results were obtained for the other diameters. As expected, impact force increased when drop height increased and trends, in the range of drop height investigated, were well explained by second order equations, with determination coefficients greater than 0.996.
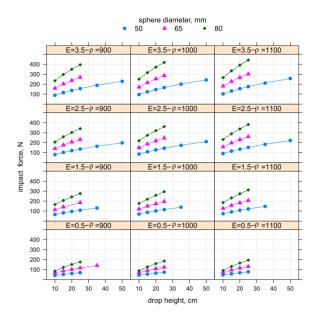

Figure 5 Maximum impact force vs. drop height at varying modulus of Young E (MPa) and density ρ (kg/m^3) for three sphere diameters.

In a previous work, Geyer et al. (2009) reported that, when dropping potato tubers with mass in the range 100–210 g from 10 cm and 25 cm on steel plate, the maximum impact force was on average about 140 and 250 N respectively. These simulations, in similar conditions (mass = 102–199 g, modulus of Young = 2.5–3.5 MPa, density = 900–1100 kg/m^3), provided maximum impact forces of 154 N and 271 N, in good agreement with the experimental results.

Similar trends were obtained when considering the maximum acceleration at the centre of the sphere (Figure 6), with determination coefficients greater than 0.976.
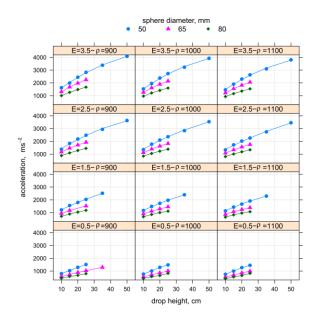

Figure 6 Maximum acceleration vs. drop height at varying modulus of Young E (MPa) and density ρ (kg/m^3) for three sphere diameters.

In the cited work, Geyer et al. (2009) reported maximum acceleration values at the centre of the potatoes, measured with the AMU device in the aforementioned conditions, of around 50 g (490 m/s^2) for drop heights of 10 cm and of around 80 g (785 m/s^2) for drop heights of 25 cm. Simulations, instead, provided average values of acceleration about 2.4 times greater (1200 m/s^2 with drop height of 10 cm and 2000 m/s^2 with drop height of 25 cm).

This difference could be due to imperfect fit of implantation system of the AMU device inside the tuber. The implant cannot be fixed tightly inside the fruit and has therefore uncontrolled movements relative to the fruit, which may cause a damping effect on acceleration values. As a confirmation, dropping the IS100 'Instrumented Sphere' on steel surfaces from 8 and 24 cm, the Authors measured acceleration values of (197 ± 23) g and (367 ± 51) g respectively (mean ± standard deviation), much higher than those measured by the AMU device (Blandini et al., 2009).

3.2 Effect of modulus of Young

The trend of the average value of the impact force vs. the modulus of Young was approximately linear, with coefficient of determination $R^2 = 0.97$, significant at p-level = 0.05. When the modulus of Young increased from 0.5 up to 3.5 MPa, the average impact force

increased from 101 up to 232 N.

The trends for some sphere diameters (50, 65 and 80 mm) are shown in Figure 7. They were all linear with coefficients of determination greater than 0.916. The increase in impact force per unit increase of modulus of Young ($\Delta F/\Delta E$) ranged from 16 to 81 N/MPa, with higher values for high sphere diameters.
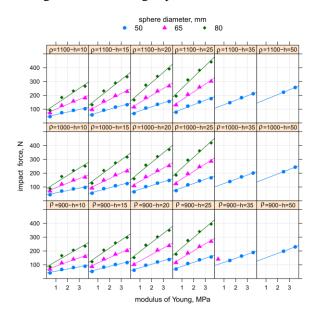

Figure 7 Maximum impact force vs. modulus of Young at varying drop height h (cm) and density ρ (kg/m^3) for three sphere diameters.

The average acceleration at the centre of the sphere also increased linearly with the modulus of Young (coefficient of determination equal to 0.98, significant at p-level = 0.01). When the modulus of Young increased from 0.5 to 3.5 MPa, the acceleration increased from 926 to 1940 m/s^2. The increase in acceleration (m/s^2) per unit increase in modulus of Young (MPa) was on average 341 m/s^2/MPa.

The trends of acceleration for some sphere diameters (50, 65, 80 mm) at varying material density and drop height are reported in Figure 8.
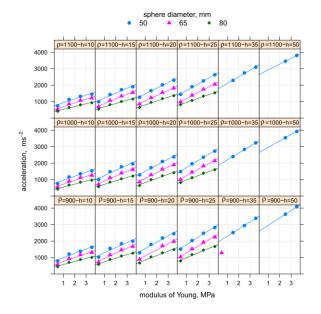

Figure 8 Maximum acceleration vs. modulus of Young at varying drop height h (cm) and density ρ (kg/m^3) for three sphere diameters.

All trends were linearly increasing, with coefficients of determination greater than 0.743. The increase in maximum acceleration per unit increase of modulus of Young ranged from 122 to 594 (m/s^2)/MPa, with higher values for high drop heights.

3.3 Effect of diameter

The effect of the sphere diameter on the impact force is shown in Figure 9 at varying drop height and modulus of Young when the material density was 1000 kg/m^3. Similar graphs were obtained when the material density was changed.
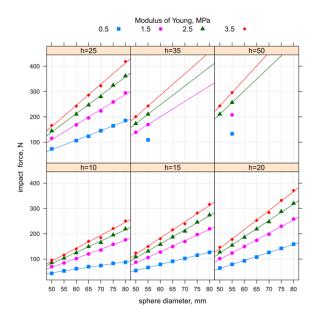
Figure 9 Maximum impact force vs. sphere diameter at varying drop height h (cm) and modulus of Young when the material density was 1000 kg/m^3.

Figure 10 Maximum acceleration vs. sphere diameter at varying drop height h (cm) and modulus of Young when the material density was 1000 kg/m^3.

The trends were linearly increasing, with coefficients of determination greater than 0.946. Slopes increased at increasing drop height, modulus of Young and density from 1.5 N/mm up to 11.1 N/mm. As an example, when the drop height was 25 cm and the material density was 1100 kg/m^3, the impact force increased from 77 N (diameter of 50 mm) to 194 N (diameter of 80 mm) when the modulus of Young was 0.5 MPa and from 176 N to 442 N when it was 3.5 MPa.

The maximum acceleration values at the centre of the sphere are represented in Figure 10 for material density equal to 1000 kg/m^3.
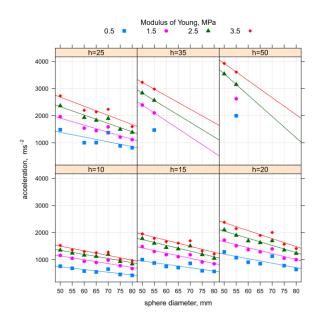
They showed a linear decreasing trend, due to the cushioning effect produced by the sphere material itself: when the size of the sphere increased, there was a greater distance between impact zone and centre of the sphere, so the acceleration measured at the centre of the sphere was reduced.

3.4 Effect of material density

The effect of the material density on impact force and acceleration is shown in Figure 11 and Figure 12 when the modulus of Young was 3.5 MPa. Similar graphs were obtained for the other values of the modulus of Young.
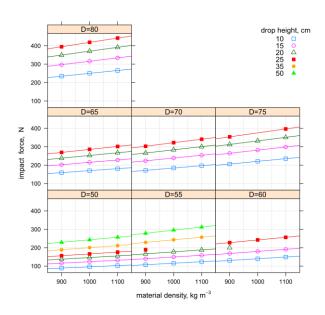
Figure 11 Maximum impact force vs. material density at varying sphere diameter D (cm) and drop height when the modulus of Young was 3.5 MPa.
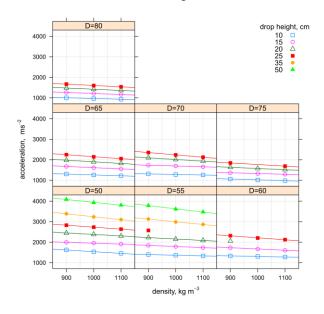

Figure 12 Maximum acceleration vs. material density at varying sphere diameter D (cm) and drop height when the modulus of Young was 3.5 MPa.

The impact force trends were linear: increasing the material density, the maximum impact force increased proportionally. The effect was more pronounced at higher sphere diameters and higher drop heights.

The trend of the acceleration at the centre of the sphere vs. the material density was also linear (Figure 12), but in decreasing direction. Again, this result was due to the cushioning effect of the material, greater when the density was greater, keeping constant all the other parameters.

3.5 Effect of mass

Size (diameter) and density of sphere were combined in one single parameter, the mass. With the given values of diameter and density, mass values ranged from 59 to 295 g.

Figure 13 reports the impact force values at varying the mass of the sphere, assuming as parameter the modulus of Young for each drop height.
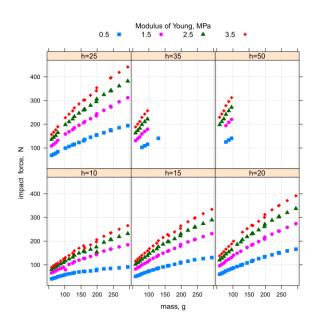

Figure 13 Maximum impact force vs. pseudo-fruit mass at varying drop height h (cm) and modulus of Young.

All trends were increasing vs. the fruit mass: fixing the drop height, the effect was more pronounced at higher modulus of Young values.

In the cited work, Geyer et al. (2009) reported that, when dropping potato tubers with mass of 100–120 g from 25 cm onto steel plates, the impact force ranged from 190 to 220 N (depending on the potato variety). Simulations showed that the impact force in similar conditions (mass of 102–113 g and modulus of Young of 2.5–3.5 MPa) ranged from 198 to 242 N, in good agreement with the experimental results. When the mass tuber was 190–210 g, the measured impact force was 310–325 N. The simulations showed that, for mass of 199–221 g, impact forces ranged from 306 to 325 N, thus in good agreement with the experimental results again.

Finally, Figure 14 reports the acceleration values at

the centre of the sphere at varying the mass of the sphere, assuming as parameter the modulus of Young for each drop height.
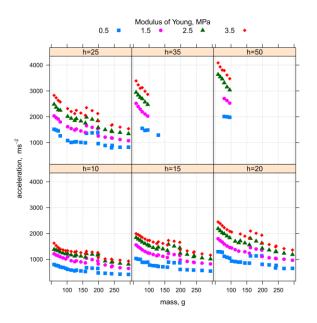

Figure 14 Maximum acceleration vs. pseudo-fruit mass at varying drop height h (cm) and modulus of Young.

The graph shows a decreasing trend in acceleration values, due to the cushioning effect of the material.

Geyer et al. (2009) reported that, in the aforementioned conditions, the acceleration measured by the AMU device ranged from 94 up to 95 g (922–932 m/s^2) for masses of 100–120 g and from 78 to 84 g (765–824 m/s^2) for masses of 190–210 g. Simulations, in similar conditions, provided acceleration values ranging from 1934 to 2314 m/s^2 for masses of 102–113 g, moduli of Young of 2.5–3.5 MPa and ranging from 1497 up to 1843 m/s^2 for masses of 199–221 g.

Simulated acceleration values were therefore about twice as high as those measured and the difference could be due, as previously said, to the implantation system of the AMU device inside the tuber.

4   Conclusions and perspectives

Impact force and acceleration arising from collisions are between the main indices that are taken into account when studying the damage of fruits and vegetables during post-harvest activities. In this study it was simulated, by means of the Finite Element Analysis approach, the behaviour of spherical fruits when dropped onto steel plates.

Even if further studies are necessary to improve the model, the main results of the simulations allow the following conclusions:

-Maximum impact force and maximum acceleration at the centre of the sphere vs. drop height, when fixing density and modulus of Young of the material and diameter of the sphere, showed increasing trends that were well explained by second order equations.

-Average value of impact force and acceleration at the centre of the sphere vs. modulus of Young showed a linear increasing trend.

-The sphere diameter had a linear effect on the impact force: fixing drop height, modulus of Young and material density, an increase in the sphere diameter caused a linear increase in the maximum impact force. The maximum acceleration at the centre of the sphere vs. sphere diameter, instead, reported a linear decreasing trend, due to the cushioning effect produced by the sphere material itself: when the size of the sphere increased, there was a greater distance between impact zone and the centre of the sphere, so the acceleration measured at the centre of the sphere was reduced.

-The trends of the maximum impact force vs. material density were linear: increasing material density, maximum impact force increased proportionally. The effect was more pronounced at higher sphere diameters and higher drop heights. The trends of the acceleration at the centre of the sphere vs. material density were also linear, but in decreasing direction. Again, this result was due to the cushioning effect of the material, greater when the material density was greater, keeping constant all the other parameters.

-Combining diameter and density of the sphere in one single parameter, the mass of the sphere, the simulations showed an increasing trend of the maximum impact force vs. the mass. The acceleration values at the centre of the sphere at varying the mass of the sphere and assuming as parameters the modulus of Young, reported a decreasing trend for each drop height, due to the cushioning effect of the material.

-Simulated impact force values were in good

agreement with experimental results reported in literature, referred to potato tubers dropped in similar conditions. Simulated acceleration values were instead about twice as high as those measured in the experimental results and this difference could be due to the imperfect fit of the implantation system of the acceleration sensor inside the tuber.

Considering all, the results obtained confirmed the validity of the FEM approach, although the limitations owing to the simplicity of the model developed in this work. Further development of the work should take into account:

-implementation of other simulations with more complex models that better represent the specific material of vegetables;

-development of other simulations on other types of vegetables to validate the method of analysis.

Acknowledgements

References

ASAE Standards. 1999. S368.3: Compression test of food materials of convex shape. St. Joseph, Mich.: *ASAE*.

Baritelle, A. L., and G. M. Hyde. 2001. Commodity conditioning to reduce impact bruising. Postharvest Biology and Technology, 21(2001): 331–339.

Bentini, M., C. Caprara, and R. Martelli. 2008. Evaluation of the physical-mechanical properties of potatoes during conservation. International Conference "Innovation Technology to Empower Safety, Health and Welfare in Agriculture and Agro-food Systems", Ragusa, Italy, 15–17 September.

Bielza, C., P. Barreiro, M. I. Rodríguez-Galiano, and J. Martín. 2003. Logistic regression for simulating damage occurrence on a fruit grading line. Computers and Electronics in Agriculture, 39(2003): 95–113.

Blandini, G., E. Cerruto, G. Manetto, and E. Romano. 2003. Mechanical damage to oranges caused by repeated impact against steel. XXX CIOSTA – CIGR V Congress, 1: 400–407. Turin, 22–24 September.

Blandini, G., E. Cerruto, and G. Manetto. 2002. Investigation on the mechanical damage of oranges in packing lines.

Riv. di Ing. Agr., 2(2002): 1–12.

Dintwa, E., M. Van Zeebroeck, H. Ramon, and E. Tijskens. 2008. Finite element analysis of the dynamic collision of apple fruit. Postharvest Biology and Technology, 49(2008): 260–276.

Di Renzo, G. C., G. Altieri, F. Genovese, and C. D'Antonio. 2009. A method to set-up calibration curve for instrumented sphere IS100 to control mechanical damage during post-harvesting and handling of oranges. J. of Ag. Eng. - Riv. di Ing. Agr., 4(2009): 9–17.

Eissa, A. H. A., N. S. Albaloushi, and M. M. Azam. 2013. Vibration analysis influence during crisis transport of the quality of fresh fruit on food security. Agric Eng Int: CIGR Journal, 15(3): 181–190.

Geyer, M. O., U. Praeger, C. König, A. Graf, I. Truppel, O. Schlüter, and B. Herold. 2009. Measuring behaviour of an acceleration measuring unit implanted in potatoes. Transactions of the ASABE, 52(4): 1267–1274.

Herold, B., I. Truppel, G. Siering, and M. Geyer. 1996. A pressure measuring sphere for monitoring handling of fruit and vegetables. Comput. Electron. Agric., 15(1996): 73–88.

Idah, P. A., M. G. Yisa, O. Chukwu, and O. O. Morenikeji. 2012. Simulated transport damage study on fresh tomato (Lycopersicon esculentum) fruits. Agric Eng Int: CIGR Journal, 14(2): 119–126.

Mohsenin, N. N. 1986. Physical properties of plant and animal materials. New York: Gordon and Breach, 2nd ed.

Opara, U. L., and P. B. Pathare. 2014. Bruise damage measurement and analysis of fresh horticultural produce—A review. Postharvest Biology and Technology, 91(2014): 9–24.

Ortiz-Cañavate, J., F. J. García-Ramos, and M. Ruiz-Altisent. 2001. Characterization of a right angle transfer point in a fruit packing line. J. agric. Engng Res., 79(2): 205–211.

Praeger, U., J. Surdilovic, I. Truppel, B. Herold, and M. Geyer. 2013. Comparison of electronic fruits for impact detection on a laboratory scale. Sensors, 13(2013): 7140–7155.

R Core Team. 2013. R: A language and environment for statistical computing.:R Foundation for Statistical Computing, Vienna, Austria. Available at: http://www.R-project.org/. Accessed 16 January 2014.

Ragni, L., and A. Berardinelli. 2001. Mechanical behaviour of apples and damage during sorting and packaging. J. Agric. Eng. Res., 78(2001): 273–279.

Rao, M. A., S. S. H. Rizvi, and A. K. Datta. 2005. Engineering properties of foods, Boca Raton, FL: CRC Press, Taylor & Francis Group, 3rd ed.

Shahbazi, F., M. Geyer, U. Praeger, C. König, and B. Herold. 2011. Comparison of two impacts detecting devices to measure impact load on potatoes. Agric Eng Int: CIGR Journal, 13(1): 1–6.

Studman, C. J. 2001. Computers and electronics in postharvest technology—a review. Computers and Electronics in Agriculture, 30(2001): 109–124.

Van Canneyt, T., E. Tijskens, H. Ramon, R. Verschoore, and B. Sonck. 2003. Characterisation of a potato-shaped instrumented device. Biosystems Engineering, 86(3): 275–285.

Zapp, H. R., S. H. Ehlert, G. K. Brown, P. R. Armstrong, and S. S. Sober. 1990. Advanced Instrumented Sphere (IS) for Impact Measurements. Transaction of the ASAE, 33(3): 955–960.